Cell Reports, Volume *37*

Supplemental information

A potent bispecific nanobody protects hACE2 mice against SARS-CoV-2 infection via intranasal administration

Xilin Wu, Lin Cheng, Ming Fu, Bilian Huang, Linjing Zhu, Shijie Xu, Haixia Shi, Doudou Zhang, Huanyun Yuan, Waqas Nawaz, Ping Yang, Qinxue Hu, Yalan Liu, and Zhiwei Wu

This file includes:

Supplemental Figures 1 to 7

Supplemental Table 1 to 3

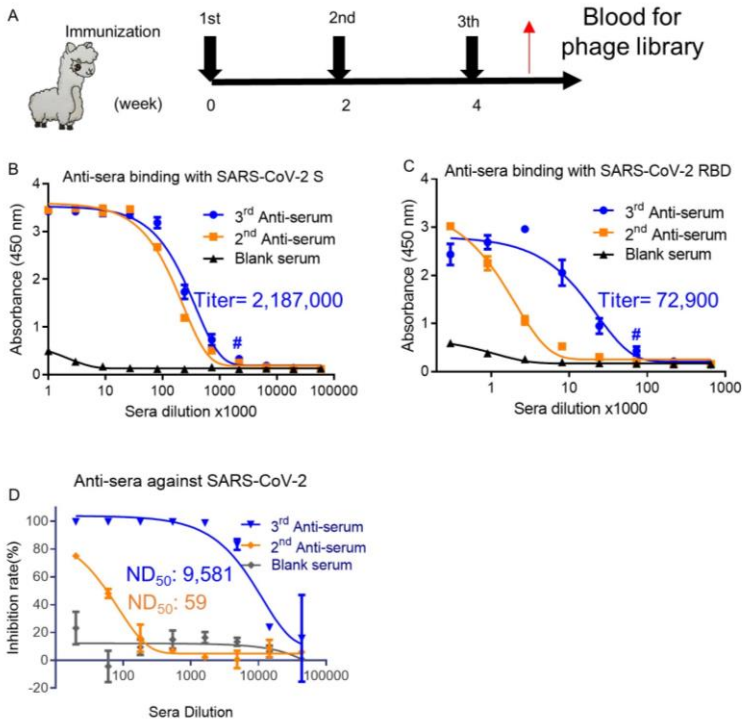

Supplemental Figure 1. Characterization of anti-sera specific for SARS-CoV-2. **Related to Figure 1.** (**A**) The experimental schedule for immunization. The titer of anti-sera specific for SARS-CoV-2 S protein (**B**) and RBD protein (**C**) was evaluated one week after the immunization in alpaca receiving SARS-CoV-2 spike protein, respectively. The titer of the third anti-serum was indicated as blue line. The blue # indicates the anti-serum titer after the third immunization. 3rd anti-serum and 2nd anti-serum represent the anti-sera collected from alpaca one week after the 3rd and 2nd immunization. Blank serum represents the alpaca serum collected before immunization, which was taken as a negative control. (**D**) Neutralization potency of the immunized alpaca's serum against pseudotyped SARS-CoV-2 was detected. ND_{50}: half-maximal serum neutralization dilution titer. Titer and ND_{50} were indicated. Data of B-D represent as mean ± SEM. All experiments of B-D were repeated twice.

A

The summary of C9-Nb library

Name	Library size	Sequencing clone	Sequence results	In frame clone	Diversity	In frame rate
C9-Nb-lib	2.0*10^9	25	25	24	24/24 100%	24/25 96%

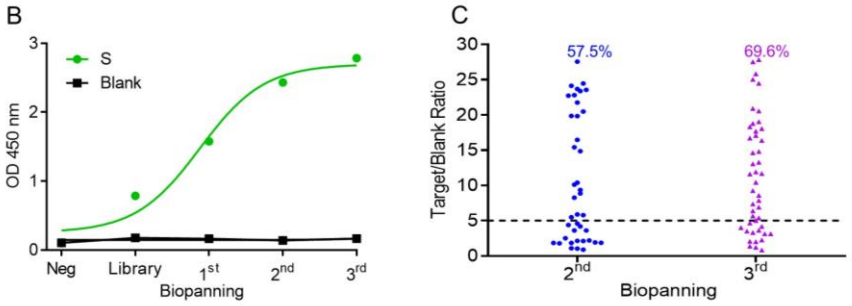

Supplemental Figure 2. The construction and biopanning of C9-Nb library. Related to Figure 1. (**A**) The table summary of C9-Nb library, wherein phage displayed Nb of PBMC from alpaca receiving three times immunization of SARS-CoV-2 S protein. (**B**) The binding of the phage library with S via phage ELISA. Lib is the phage library of C9-Nb; 1st, 2nd, and 3rd are the phage library after panning on 1 round, 2 rounds, and 3 rounds of S protein enrichment, respectively. (**C**) Single clone of phages from the C9-Nb library after the second and third enrichment of SARS-CoV-2 S were analyzed by phage ELISA. One dot represents the supernatant binding of one clone. Positive rate was indicated.

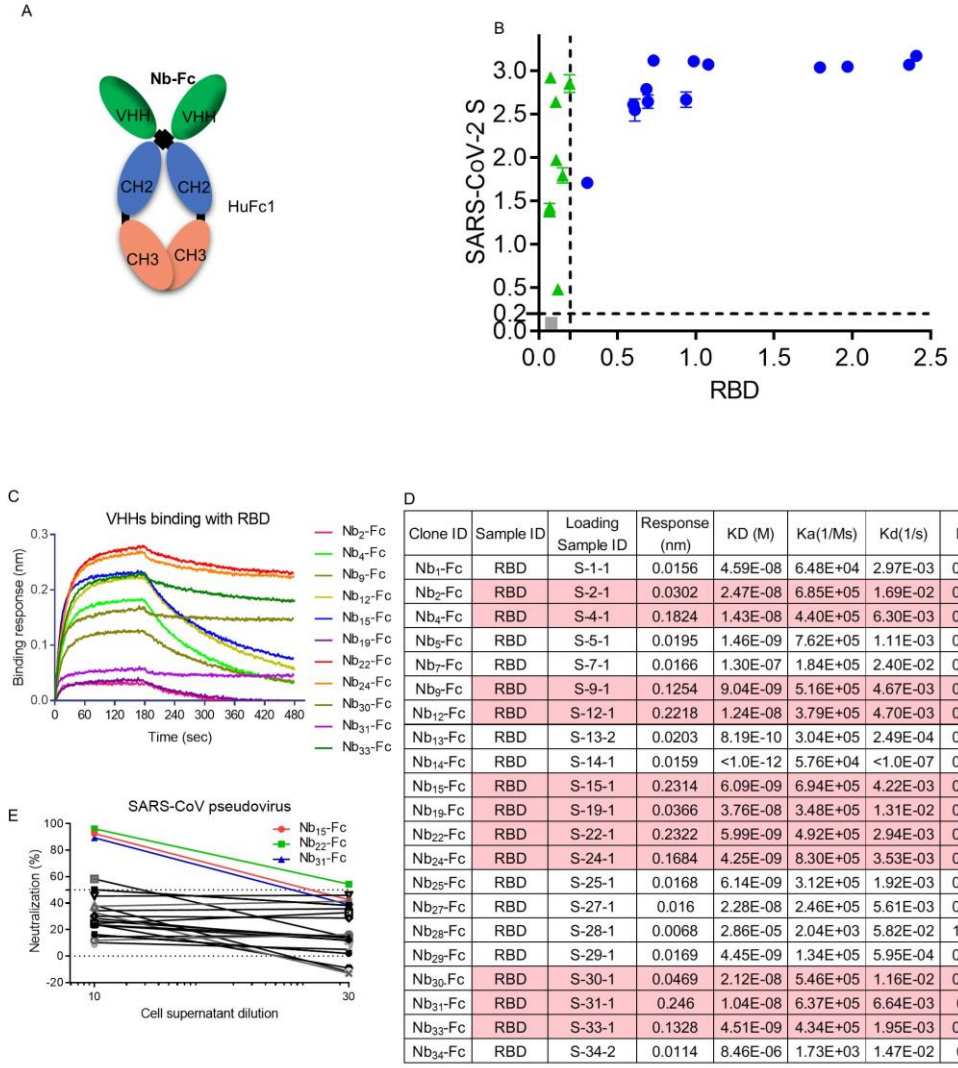

D

Clone ID	Sample ID	Loading Sample ID	Response (nm)	KD (M)	Ka(1/Ms)	Kd(1/s)	RMax	Full R^2
Nb_1-Fc	RBD	S-1-1	0.0156	4.59E-08	6.48E+04	2.97E-03	0.0274	0.862
Nb_2-Fc	RBD	S-2-1	0.0302	2.47E-08	6.85E+05	1.69E-02	0.0389	0.9273
Nb_4-Fc	RBD	S-4-1	0.1824	1.43E-08	4.40E+05	6.30E-03	0.2024	0.9956
Nb_5-Fc	RBD	S-5-1	0.0195	1.46E-09	7.62E+05	1.11E-03	0.0176	0.3834
Nb_7-Fc	RBD	S-7-1	0.0166	1.30E-07	1.84E+05	2.40E-02	0.0432	0.7633
Nb_9-Fc	RBD	S-9-1	0.1254	9.04E-09	5.16E+05	4.67E-03	0.1327	0.9938
Nb_{12}-Fc	RBD	S-12-1	0.2218	1.24E-08	3.79E+05	4.70E-03	0.2443	0.9966
Nb_{13}-Fc	RBD	S-13-2	0.0203	8.19E-10	3.04E+05	2.49E-04	0.0192	0.5595
Nb_{14}-Fc	RBD	S-14-1	0.0159	<1.0E-12	5.76E+04	<1.0E-07	0.0271	0.8809
Nb_{15}-Fc	RBD	S-15-1	0.2314	6.09E-09	6.94E+05	4.22E-03	0.2366	0.9879
Nb_{19}-Fc	RBD	S-19-1	0.0366	3.76E-08	3.48E+05	1.31E-02	0.0493	0.9862
Nb_{22}-Fc	RBD	S-22-1	0.2322	5.99E-09	4.92E+05	2.94E-03	0.2367	0.9927
Nb_{24}-Fc	RBD	S-24-1	0.1684	4.25E-09	8.30E+05	3.53E-03	0.1706	0.9876
Nb_{25}-Fc	RBD	S-25-1	0.0168	6.14E-09	3.12E+05	1.92E-03	0.0169	0.5564
Nb_{27}-Fc	RBD	S-27-1	0.016	2.28E-08	2.46E+05	5.61E-03	0.0199	0.8945
Nb_{28}-Fc	RBD	S-28-1	0.0068	2.86E-05	2.04E+03	5.82E-02	1.7237	0.3166
Nb_{29}-Fc	RBD	S-29-1	0.0169	4.45E-09	1.34E+05	5.95E-04	0.0204	0.8342
Nb_{30}-Fc	RBD	S-30-1	0.0469	2.12E-08	5.46E+05	1.16E-02	0.0525	0.9855
Nb_{31}-Fc	RBD	S-31-1	0.246	1.04E-08	6.37E+05	6.64E-03	0.261	0.9823
Nb_{33}-Fc	RBD	S-33-1	0.1328	4.51E-09	4.34E+05	1.95E-03	0.1364	0.994
Nb_{34}-Fc	RBD	S-34-2	0.0114	8.46E-06	1.73E+03	1.47E-02	0.975	0.8974

Supplemental Figure 3. Characterization of Nb-Fc. Related to Figure 1. (**A**) The diagram of Nb-Fc, constituted by Nb fusing with human Fc1. (**B**) 21 various Nb-Fcs binding with S and RBD protein identified by ELISA. Grey dot represents negative control. Green dots represent the specific binding with S protein. Blue dots represent the double binding with S and RBD protein. (C) Representative binding curve of Nb-Fcs with RBD tested by BLI. (**D**) The table summary of 21 Nb-Fcs binding with RBD tested by BLI. (**E**) The cell supernatants of 21 various Nb-Fcs were tested for neutralization against SARS-CoV-2 infection, the cell supernatant displaying outstanding neutralizing curve was labeled as the color-coded curve. Data of B represent as mean ± SEM. All experiments of B-E were repeated twice

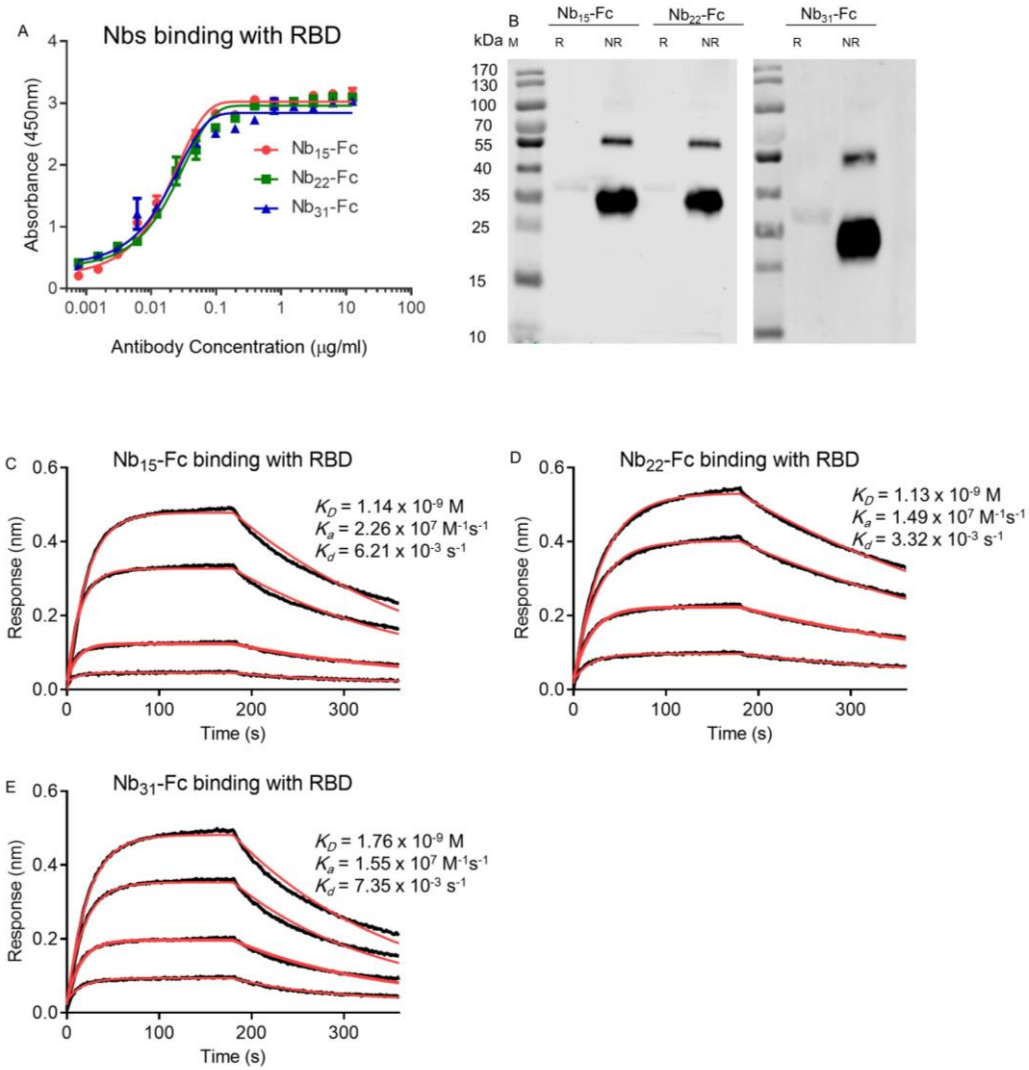

Supplemental Figure 4. Characterization of purified Nb-Fcs. Related to Figure 1. (**A**) Purified Nb-Fcs binding with RBD identified by ELISA. Data represent as mean ± SEM. (**B**) RBD protein under reducing condition (R) or non-reducing condition (NR) was detected by WB with Nb_{15}-Fc, Nb_{22}-Fc and Nb_{31}-Fc. Kinetic binding curve of RBD with Nb_{15}-Fc (**C**), Nb_{22}-Fc (**D**) and Nb_{31}-Fc (**E**), respectively. Binding curves are colored black, and fit of the data to a 1:1 binding model is colored red.

Fig. S5

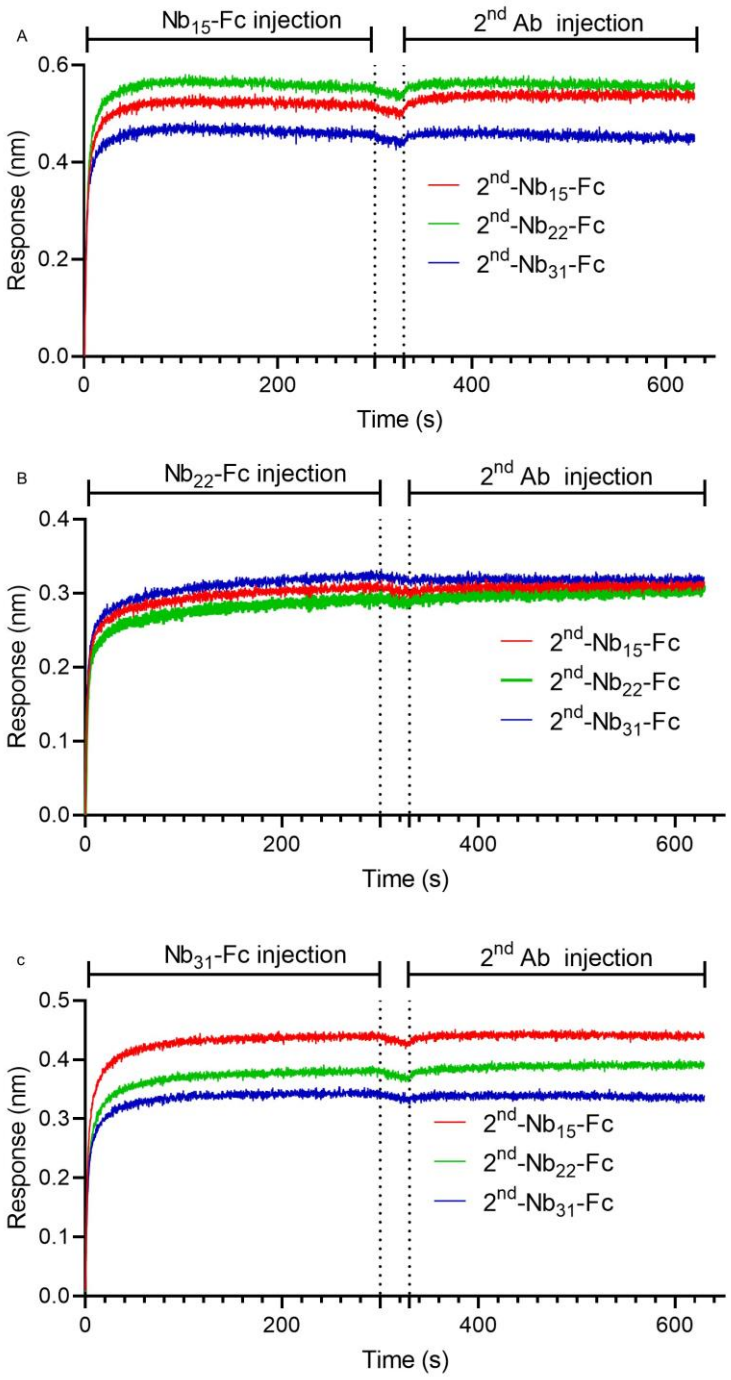

Supplemental Figure 5. Epitope analysis of Nb-Fcs by BLI. Related to Figure 1. RBD protein was coated on the sensor, Nb_{15}-Fc (**A**), Nb_{22}-Fc (**B**) or Nb_{31}-Fc(C) as the first antibody was added to bind for 300 s following with the baseline step with 30 s immersion in 0.02% PBST. The second competing concentration of Nb (50 μg/ml) was then added for 300 sec to measure binding in the presence of the first saturating Nb.

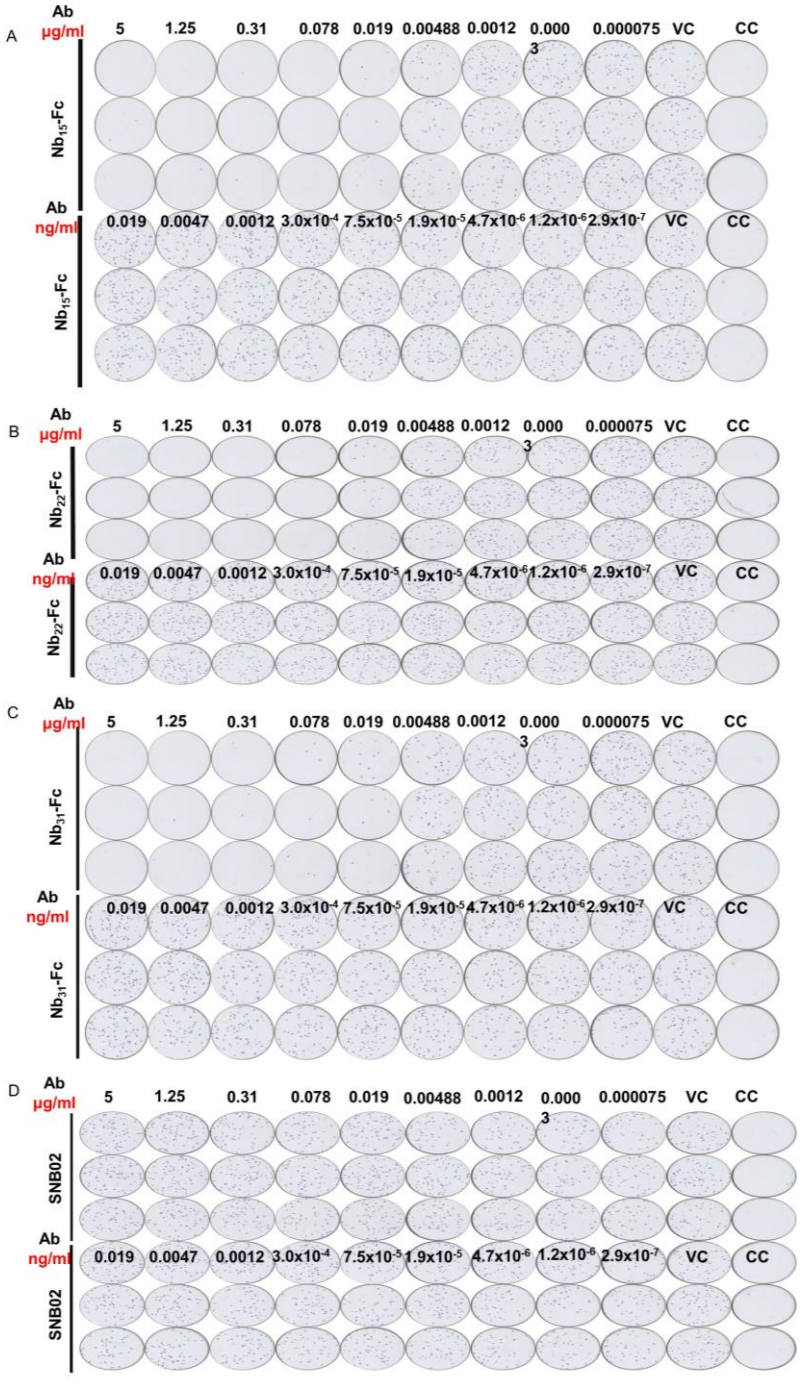

E Summary of C9Nbs inhibiting SARS-CoV-2 live virus

μg/ml	SARS-CoV-2 live virus		
	IC_{50}	IC_{80}	IC_{90}
Nb_{15}-Fc	0.0033	0.0084	0.0156
Nb_{22}-Fc	0.0068	0.0108	0.0159
Nb_{31}-Fc	0.0036	0.0100	0.0235

Supplemental Figure S6. Characterizing the potency of neutralization against authentic SARS-CoV-2 conferred by Nb-Fcs. Related to Figure 1. The neutralization potency of Nb_{15}-Fc (**A**), Nb_{22}-Fc (**B**), Nb_{31}-Fc(**C**), SNB02 (isotype control antibody) (**D**) was detected based on authentic SARS-CoV-2 plaque reduction neutralization test. The raw data was depicted. (**E**) A table summary authentic SARS-CoV-2 neutralization potencies of Nb-Fcs.

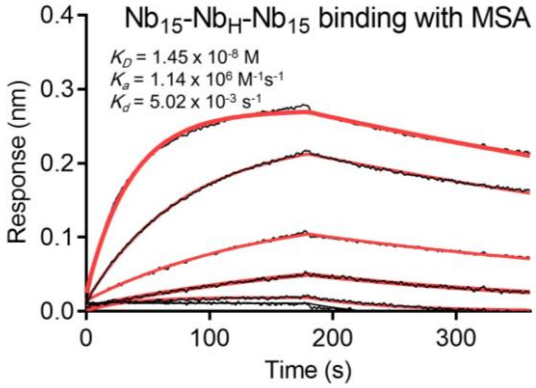

Supplemental Figure 7. Kinetic binding curve of Nb_{15}-Nb_H-Nb_{15} with MSA. Related to Figure 5.

Kinetic binding curve of Nb_{15}-Nb_H-Nb_{15} at the concentration of 300 nM, 100nM, 33.3 nM,11.1nM, 3.7nM and 1.2 nM with MSA by BLI. Binding curves are colored black, and fit of the data to a 1:1 binding model is colored red.

Supplemental Table 1. Summary of CDR sequences of positive Nb clones. Related to Figure 1.

ID	CDR1	CDR2	CDR3
Nb_1-Fc	GNIFSIYT	VTSGGST	N----------ARLFDPGY
Nb_2-Fc	GGTLASFA	INIINRT	AAHFVPPGSRLRDCLVNELYNY
Nb_4-Fc	GGTLASFA	INIINRT	AAHFVPPGSRLRGCLVNELYNY
Nb5-Fc	GFTWNYHA	ISSSGSTT	AAPHSGSVCPR--WAEYYGVDH
Nb_7-Fc	GGTLASFA	INIINRT	AAHFVPPGSRLRGCLVNEAYNY
Nb9-Fc	GGTLASFA	INIINRT	AAHFVPPGGRLRGCLVNDLYNY
Nb_{12}-Fc	GGTLASFA	INIINRT	AAHFVPPGSRLRGCLVNDLYNY
Nb_{13}-Fc	GGTLASFA	ITNSGST	N----------TFHY
Nb_{14}-Fc	GGTLASFA	ISSSGGST	TARPSLWAVVAGCPLDQNTYFS
Nb_{15}-Fc	GGTLASFA	ISSSGST	AG-VVHDVQAM--CVMNP-WGS
Nb_{19}-Fc	GGTLASFA	INIINRT	AAHFVPPGSRLRGCLVNDVYNY
Nb_{22}-Fc	GGTLASFA	IDVINRA	AAHFVPPGSRLRGCLVNELYNY
Nb_{24}-Fc	GGTLASFA	INIINRT	AAHFVPPESRLRGCLVNELYNY
Nb_{25}-Fc	GGTLASFA	ITSRRDT	YG----------QDVLGQIY
Nb_{27}-Fc	GGTLASFA	ITSGGST	TT----------AGSWQGDY
Nb_{28}-Fc	GGTLASFA	INIINRT	AAHFVPPESRLRGCLVNEAYNY
Nb_{29}-Fc	GGTLASFA	ISSRSFT	YG----------QDILGQIY
Nb_{30}-Fc	GGTLASFA	INIINRT	AAHFVPPGSRLRGCLVNELYNY
Nb_{31}-Fc	GGTLASFA	INIINRP	AAHFVPPGSRLGGCLVNELYNY
Nb_{33}-Fc	GGTLASFA	INIINRT	AAHFVPPGSRFRGCSVNELYNY
Nb_{34}-Fc	GGTLASFA	INIINRP	AAHFVPPGSRLGGCLVNELYNY
Nb_H	GFILDYYA	IDSSGGTT	AAGGDLGVGQCSTWVRAYDY

Supplemental Table 2. Summary of Nbs inhibiting SARS-CoV-2 variants. Related to Figure 1.

Variants	Nb_{15}-Fc (mean±sd μg/ml)			Nb_{22}-Fc (mean±sd μg/ml)			Nb_{31}-Fc (mean±sd μg/ml)			Nb_{15}-Nb_H-Nb_{15} (mean±sd μg/ml)		
	IC_{50}	IC_{80}	IC_{90}	IC_{50}	IC_{80}	IC_{90}	IC_{50}	IC_{80}	IC_{90}	IC_{50}	IC_{80}	IC_{90}
WT	0.0008±0.0001	0.0019±0.0004	0.0033±0.0012	0.0016±0.0001	0.0046±0.0012	0.0086±0.0033	0.0023±0.0004	0.0083±0.0019	0.0183±0.0059	0.0004±0	0.0012±0.0004	0.0018±0.0009
Q321L	0.0009±0.0004	0.0023±0.0007	0.0039±0.0008	0.0014±0.0003	0.0042±0.0009	0.0079±0.0019	0.002±0.0005	0.0065±0.0017	0.0133±0.0033	0.001±0.0001	0.0022±0.0004	0.0034±0.0009
V341I	0.0007±0.0002	0.0026±0.0005	0.0059±0.0019	0.0017±0.0005	0.0042±0.0007	0.007±0.001	0.0028±0.0004	0.0087±0.0024	0.0169±0.0058	0.0011±0.0001	0.0027±0.0009	0.0047±0.0022
A348T	0.001±0.0002	0.0023±0.0003	0.0036±0.0005	0.0019±0.0008	0.0046±0.0012	0.0076±0.0016	0.0029±0.0001	0.0088±0.0013	0.0176±0.0032	0.0008±0.0002	0.0014±0.0001	0.0019±0.0004
N354D	0.0008±0.0002	0.0022±0.0002	0.0041±0.001	0.0013±0.0003	0.0033±0.0005	0.0056±0.0012	0.0019±0.0001	0.0068±0.0018	0.0145±0.0051	0.0006±0.0002	0.0016±0.0006	0.0032±0.0013
S359N	0.0011±0.0001	0.0026±0.0003	0.0043±0.0006	0.0016±0.0003	0.0037±0.0005	0.0061±0.0008	0.002±0.0005	0.0064±0.0012	0.0129±0.0037	0.0008±0.0002	0.0017±0.0002	0.0025±0.0005
V367F	0.0007±0.0001	0.002±0.0002	0.0036±0.0004	0.0011±0.0003	0.0033±0.0003	0.0062±0.0004	0.0021±0.0006	0.0095±0.0017	0.0237±0.0022	0.0005±0	0.0013±0.0001	0.0026±0.0006
K378R	0.0007±0.0002	0.0024±0.0003	0.0046±0.0001	0.0012±0.0002	0.0028±0.0003	0.0045±0.0005	0.0013±0.0001	0.004±0.0004	0.0079±0.0017	0.0008±0.0002	0.002±0.0004	0.0033±0.0006
R408I	0.0007±0.0002	0.002±0.0007	0.0035±0.0016	0.001±0.0001	0.0027±0.0003	0.0047±0.0009	0.0014±0.0002	0.0038±0.001	0.0069±0.0026	0.0007±0.0001	0.0014±0.0002	0.002±0.0005
Q409E	0.0005±0.0001	0.0014±0	0.0026±0.0002	0.0009±0.0003	0.0022±0.0007	0.0036±0.0011	0.0009±0.0001	0.0029±0.0004	0.0057±0.0007	0.0007±0.0002	0.0014±0.0002	0.0021±0.0003
K458R	0.0009±0.0003	0.0025±0.0002	0.0047±0.0006	0.0013±0.0001	0.0041±0.0014	0.008±0.0036	0.0025±0.0003	0.0068±0.0013	0.0128±0.004	0.0008±0.0002	0.0018±0.0003	0.0029±0.0004
G476S	0.0006±0.0002	0.0015±0.0004	0.0025±0.0006	0.0013±0.0006	0.0034±0.0011	0.006±0.0013	0.0015±0.0001	0.0049±0.0008	0.0101±0.0023	0.0003±0.0001	0.0009±0.0002	0.0014±0.0003
V483A	0.0006±0.0001	0.0017±0.0005	0.0031±0.0011	0.0015±0.0003	0.0039±0.0008	0.0069±0.0026	0.0027±0.001	0.0093±0.0018	0.0206±0.0027	0.0005±0.0001	0.0013±0	0.0022±0.0002
Y508H	0.0005±0.0001	0.0023±0.0003	0.0053±0.001	0.0013±0.0002	0.0035±0.0007	0.006±0.0015	0.0018±0.0005	0.0068±0.0007	0.0157±0.0047	0.0008±0.0001	0.0019±0.0006	0.0033±0.0016
H519P	0.0008±0.0001	0.0023±0.0002	0.0041±0.0005	0.0011±0.0002	0.0033±0	0.006±0.0004	0.0014±0.0003	0.005±0.0004	0.0107±0.0032	0.0007±0.0002	0.0016±0.0001	0.0025±0.0002
D614G	0.0007±0.0001	0.002±0.0002	0.0035±0.0007	0.0012±0.0005	0.0033±0.0005	0.0059±0.0003	0.0015±0.0004	0.0039±0.001	0.0067±0.0016	0.0006±0.0001	0.0015±0.0005	0.0026±0.001
A435S	N/A	N/A	N/A	N/A	N/A	N/A	N/A	N/A	N/A	0.0007±0.0001	0.0015±0.0003	0.0024±0.0006
I472V	N/A	N/A	N/A	N/A	N/A	N/A	N/A	N/A	N/A	0.0006±0.0001	0.0014±0.0003	0.0023±0.0006
E484K	N/A	N/A	N/A	N/A	N/A	N/A	N/A	N/A	N/A	>1.000	>1.000	>1.000
N501Y	N/A	N/A	N/A	N/A	N/A	N/A	N/A	N/A	N/A	0.0007±0.0002	0.002±0.0005	0.0042±0.0013

Note: N/A, no test

Supplemental Table 3. Summary of RBD binding with Nb_{15}s in different conditions. **Related to Figure 5.**

Sample ID	Condition	Conc. (nM)	Response	KD (M)	Ka(1/Ms)	Kd(1/s)	RMax	Full R^2
Nb_{15}-Nb_H-Nb_{15}	WT	133.3	0.3806	<1.0E-12	3.44E+05	<1.0E-07	0.3687	0.9676
	Aero	133.3	0.2139	9.92E-09	4.11E+04	4.08E-04	0.3277	0.9957
	37 °C	133.3	0.3756	<1.0E-12	1.89E+05	<1.0E-07	0.374	0.9948
	50 °C	133.3	0.3903	5.78E-11	2.11E+05	1.22E-05	0.3849	0.996
	60 °C	133.3	0.4048	5.57E-10	1.91E+05	1.06E-04	0.402	0.9986
	70 °C	133.3	0.3775	2.52E-10	1.63E+05	4.10E-05	0.3801	0.9989
	80 °C	133.3	0.3199	5.64E-09	5.85E+04	3.30E-04	0.4193	0.9994
	90°C	133.3	0.1078	1.02E-08	2.90E+04	2.95E-04	0.211	0.9978
Nb_{15}-Fc	WT	62.5	0.8028	<1.0E-12	6.98E+05	<1.0E-07	0.7814	0.9824
	Aero	62.5	0.3398	2.79E-10	5.05E+04	1.41E-05	0.7387	0.999
	37 °C	62.5	0.8136	<1.0E-12	4.34E+05	<1.0E-07	0.804	0.9946
	50 °C	62.5	0.853	<1.0E-12	4.11E+05	<1.0E-07	0.848	0.9976
	60 °C	62.5	0.7989	4.38E-11	4.11E+05	1.80E-05	0.7944	0.9979
	70 °C	62.5	0.6126	4.95E-09	8.87E+04	4.39E-04	0.956	0.9995
	80 °C	62.5	0.2077	1.98E-08	4.16E+04	8.26E-04	0.557	0.9983
	90°C	62.5	0.1088	4.12E-08	2.76E+04	1.14E-03	0.4281	0.9978
3xNb_{15}	WT	133.3	0.3769	<1.0E-12	6.20E+05	<1.0E-07	0.3637	0.8833
	Aero	133.3	0.184	<1.0E-12	2.55E+04	<1.0E-07	0.3816	0.9946
	37 °C	133.3	0.3667	<1.0E-12	4.01E+05	<1.0E-07	0.3578	0.9563
	50 °C	133.3	0.3588	<1.0E-12	3.96E+05	<1.0E-07	0.3507	0.9583
	60 °C	133.3	0.3715	<1.0E-12	3.49E+05	<1.0E-07	0.3635	0.9717
	70 °C	133.3	0.2294	<1.0E-12	2.78E+04	<1.0E-07	0.4508	0.9975
	80 °C	133.3	0.2748	4.97E-10	4.53E+04	2.25E-05	0.4052	0.9994
	90°C	133.3	0.1294	4.87E-09	5.21E+04	2.54E-04	0.1778	0.9968